energies

MDPI

Article

Comparison of Axial Flow and Swirling Flow on Particle Pickup in Horizontal Pneumatic Conveying

Yun Ji [1,2,*], Yating Hao [1], Ning Yi [1], Tianyuan Guan [1], Dianrong Gao [1,2] and Yingna Liang [1]

[1] School of Mechanical Engineering, Yanshan University, Qinhuangdao 066004, China
[2] Hebei Provincial Key Laboratory of Heavy Machinery Fluid Power Transmission and Control, Yanshan University, Qinhuangdao 066004, China
* Correspondence: jiyun@ysu.edu.cn

Abstract: Pneumatic conveying is widely used in coal mining. As the lowest conveying velocity of materials, the pickup velocity is the key to the study of gas–solid two-phase flow. In this study, the pickup velocity of pebble particles was experimentally investigated. When the particle size is 3–9 mm, the airflow velocity was found to suitably describe the results as a function of the pickup velocity and have a high correlation. When the swirl number is 0.2, the optimal swirl number was found for which the highest particle pickup ratio was observed. Based on four different methods, namely, visual observation, mass weighing, coefficient of difference analysis, and determination of the peak-average ratio of the pressure drop in the flow field to measure the pickup velocity of the spraying material, the results showed that the accuracy of the particle pickup velocity obtained through visual observation was the lowest, and when the mass–loss rate of the particle was selected as the measurement index of the pickup velocity, the accuracy was the highest. The results will help to realize the long-distance transportation of spraying materials in inclined roadway under the shaft.

Keywords: axial flow; swirling flow; pickup behavior; coefficient of variation

Citation: Ji, Y.; Hao, Y.; Yi, N.; Guan, T.; Gao, D.; Liang, Y. Comparison of Axial Flow and Swirling Flow on Particle Pickup in Horizontal Pneumatic Conveying. *Energies* **2022**, *15*, 6126. https://doi.org/10.3390/en15176126

Academic Editors: Gan Feng, Qingxiang Meng, Gan Li and Fei Wu

Received: 7 July 2022
Accepted: 20 August 2022
Published: 23 August 2022

1. Introduction

In recent years, the construction technology for coal mining in China has developed rapidly, and the monthly footage of roadway wellbore construction has exceeded 100 m [1,2]. Roadway excavation is of great significance for coal mining. However, the conveying distance of spraying materials is less than 200 m. For a long-distance inclined shaft excavation (≥500 m), conveying the spraying materials by laying the track results in considerable safety risks and low work efficiency. Therefore, long-distance pneumatic conveying of spraying materials is of high economic value and social benefits.

Pneumatic conveying is widely used in chemical, mining, and other industries, which utilizes the airflow to convey particulate material along the direction in a closed pipeline [3,4]. In the past few years, we have devoted ourselves to the study of long-distance pipeline dilute-phase pneumatic conveying of spraying materials, and committed to applying this technology to the long-distance pipeline conveying of underground roadway gangue and coal mining [5,6]. For long-distance pipeline conveying, the pressure drop in the pipeline increases with the conveying distance, resulting in blockage of the pipeline. When the airflow velocity reaches the pickup velocity of particles, particles are disturbed and gradually picked up. Conversely, particles suspended in the pipeline gradually settle and pile up at the pipeline bottom. Researchers have investigated the threshold velocities of pneumatic systems, which can be classified into two groups: the velocity required to move these particles when they are initially moving (pickup velocity) and that to keep the particles moving and prevent them from deposition (saltation velocity).

Pickup velocity is the limit airflow velocity required to pick up the particles [7]. A few studies on pickup velocity have been conducted to reveal the basic features. Soepyan [8]

used a novel combination of various methods to predict the confidence of solid transport models by considering the input conditions, experimental data, and modified model. Rice [9] proposed a general functional form for the critical deposition velocity to analyze the low solid void fractions based on the Reynolds number and Archimedes number of particles. Gomes [10] developed an analytical model to analyze the effect of the particle size and particle shape on particle picking mechanism in a horizontal pipe and found that the pickup velocity increased with a decrease in particle sphericity. Dasani [11] measured the pickup velocity of three glass spheres in water and compared the pickup velocity trends under various particle properties for similar gas-solid phase systems. Kalman [12] presented 100 measurements of the pickup velocity of 24 materials having various particle sizes, shapes, and densities and established simple relationships of three zones between the Reynolds and Archimedes numbers (see Figure 1). However, these studies mainly involved micron-sized powder particles. For pebble particles having a size of more than 3 mm, the saltation and pickup velocity significantly differ from those of the powder. Furthermore, the main focus of the aforementioned studies was the particle pickup regimes, and how to reduce the minimum airflow velocity remains unclear. Reducing the airflow velocity can effectively reduce energy consumption, and how to reduce the particle pickup velocity is still an urgent problem to be solved.

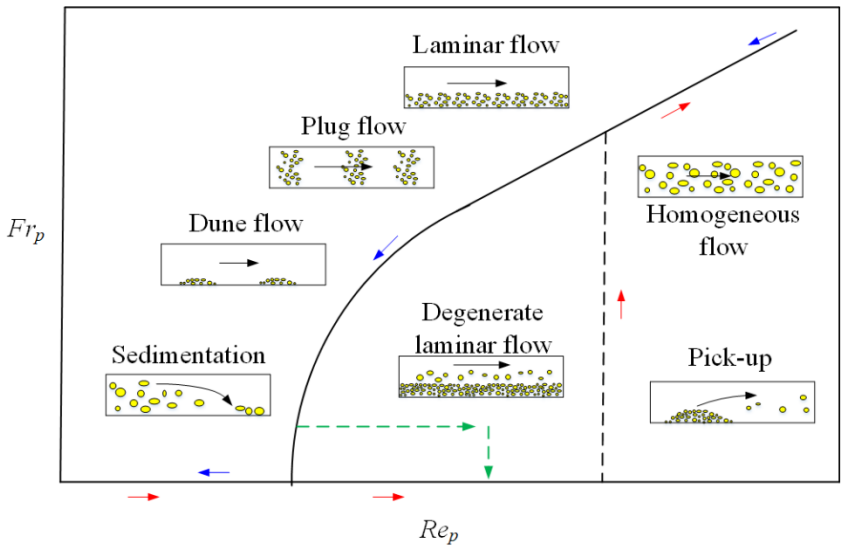

Figure 1. Model of flow regimes observed for horizontal pneumatic conveying.

Swirling pneumatic conveying can effectively reduce the pickup speed of solid particles, and researchers have carried out a lot of research on swirling pneumatic conveying. Zhou [13–15] studied the influence of the type of swirl generator and the intensity of swirl on the pickup speed of lump coal particles, and found that the swirl helps to pick up the particles from the front to the end of the particle bed. Ibrahim [16] used turbulence models to study the swirling pneumatic conveying, and found the most suitable turbulence model in a vertical dryer. Yao [17] studied laminar flow in a horizontal pipeline, focusing on the slug flow and velocity distribution in the pipeline, and studied the effect of the inlet swirl number, Reynolds number, and axial spacing on the swirl decay and velocity distribution. Fokeeret [18,19] studied the three-leaf swirling airflow, obtained the swirl intensity in the pipeline by a laser Doppler anemometer, and studied the effect of the Reynolds number and the distance from the pipeline outlet on the swirl decay. Li [20–24] studied the swirl airflow on vertical and horizontal pipes by comparing experimental results with numerical results. Zhou [25] studied the effects of swirls on gas-solid pneumatic conveying, and determined the tangential velocities of weak and strong swirls. Studies have shown that the swirling pneumatic flow is beneficial for the reduction of the conveying velocity of the solids. However, due to the interaction of the airflow-wall, the swirling flow will lead

to the swirl decay, and the coupling effect of the tangential flow and the axial flow on the particle pickup velocity will be unpredictable. Therefore, it is necessary to study the swirling pneumatic conveying for better understanding the particle picking process.

In this study, experiments were conducted to evaluate the pebble particle pickup regimes in axial and tangential flow. The effects of swirl numbers on the axial and swirl velocities in the pipeline were studied, and Gaussian fitting was performed. The airflow velocity was found to appropriately describe all the results as a function of the pickup velocity, and it had a good correlation with the results. For small particles with a diameter of 3–9 mm, Kalman's empirical equation was suitable for the particle pickup velocity, and the pickup velocity increased with the particle size. The highest pickup ratio was observed when the swirling flow number was between 0.1 and 0.2. Based on a comparison of the particle pickup velocities obtained by using four methods, namely, visual observation, mass weighing, analysis of the coefficient of difference (CV) of the pressure drop in a flow field, and determination of the peak-average ratio (PAR) of the pressure drop in a flow field, the accuracy of the particle pickup velocity obtained through visual observation was found to be the lowest, and the highest was obtained by considering the accuracy of the particle mass-loss rate as the measurement index of the pickup velocity. For pipeline pneumatic conveying, where measuring the material pickup rate is difficult, the particle pickup velocity and optimal swirling flow number can be obtained by determining the airflow pressure characteristics of the flow field, CV of the pressure signal, and PAR.

2. Experimental Setup

2.1. Experimental Materials

For particles having fixed sizes, the higher the particle density, the higher the pickup velocity. To simplify the experiment and facilitate the observation of particle flow patterns, six particles were selected by seven round screens with apertures of 3 mm, 5 mm, 7 mm, 9 mm, 11 mm, 13 mm, and 15 mm, and their sizes were 3–5 mm, 5–7 mm, 7–9 mm, 9–11 mm, 11–13 mm, and 13–15 mm, respectively. Figure 2 and Table 1 showed the results of the slump experiment of pebble particles, which were released on the surface of an acrylic plate, and the angle of repose of the pebble particle group varied from 39° to 35°. Due to the random distribution of particle size, the structure of particles was asymmetric. Larger particle sizes would result in greater angles of repose. However, the particles gradually tended to be smooth with the decrease of the size. This was because small particles accumulated more densely, and they presented better symmetry.

2.2. Experimental Apparatus

Figure 3 shows a schematic of the experimental apparatus, which were used to study the picking process of pebble particles. In the experiments, a screw air compressor was used as the source of airflow supply with 6.9 m^3/min, and its loading and unloading pressures were 0.4 MPa and 0.42 MPa, respectively. The maximum experimental airflow velocity was 200 m^3/h. The conveying pipelines used in this experiment was 50 mm; to avoid blockage in pipelines, the internal size of the pipelines should be at least three times the size of the pebble particles. An air tank was also arranged in the pipeline. In addition, it could reduce the unstable airflow generated during the loading and unloading processes. To measure the steady airflow, the stable length of the flowmeter should be at least 50 times the size of the pipeline. Therefore, the distance between the spherical valve and flowmeter was set to 70 D_{pl} in this experiment. The swirling airstream was generated when the tangential airflow passed through the swirling generator, and the particles deposited at the bottom of the pipe were disturbed at this time. The pressure sensor was installed in front of the test pipeline, and its pressure was considered as the pressure drop of the pipeline because the outlet of the pipeline was a free flow outlet, and the gauge pressure at the outlet part was approximately zero.

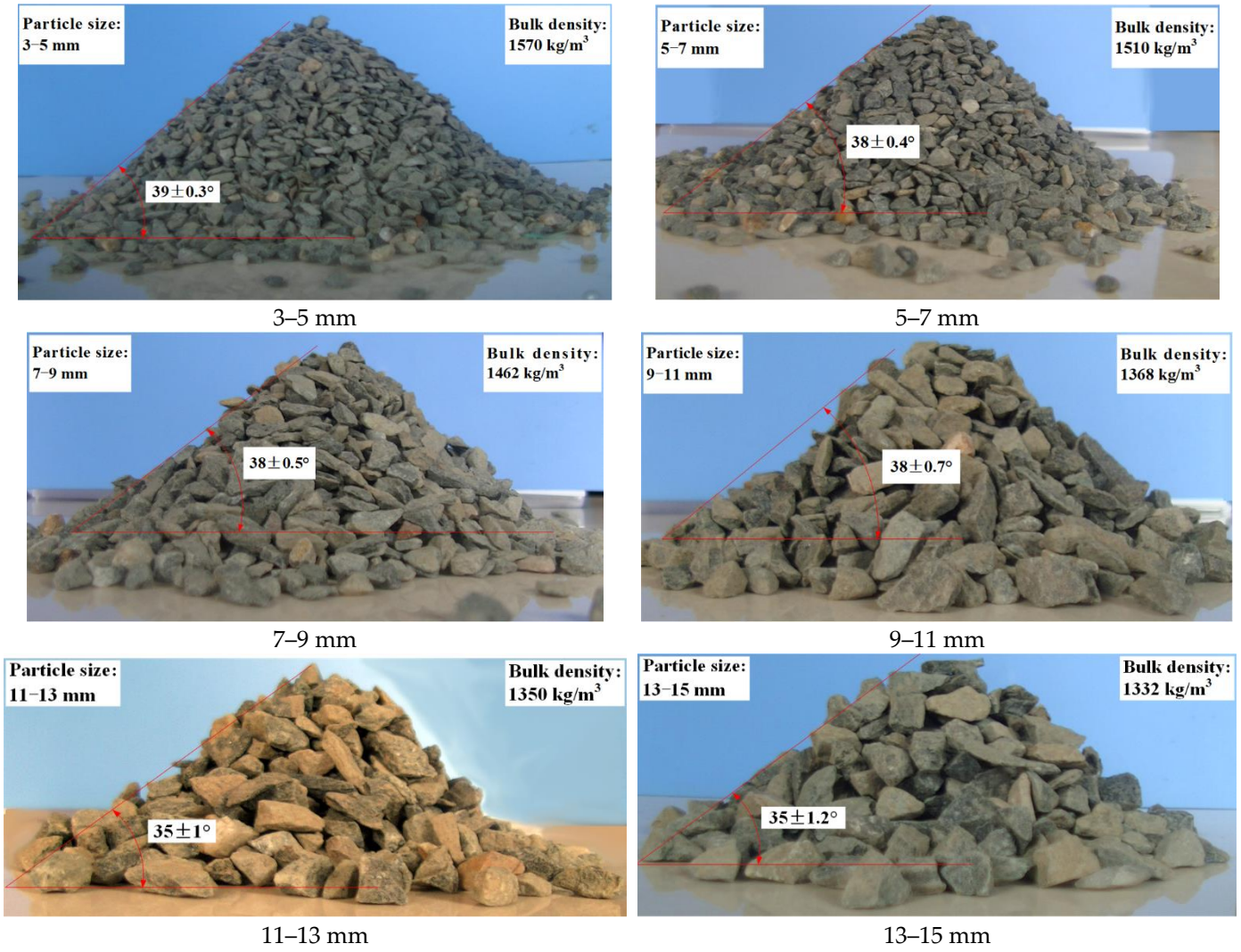

Figure 2. Slump test of pebble particles in the experiments.

Table 1. Particle sizes and their properties.

Particle size (mm)	3–5	5–7	7–9	9–11	11–13	13–15
Angle of repose (°)	39 ± 0.3°	38 ± 0.4°	38 ± 0.5°	38 ± 0.7°	35 ± 1°	35 ± 1.2°
Bulk density (kg/m^3)	1570	1510	1462	1368	1350	1332

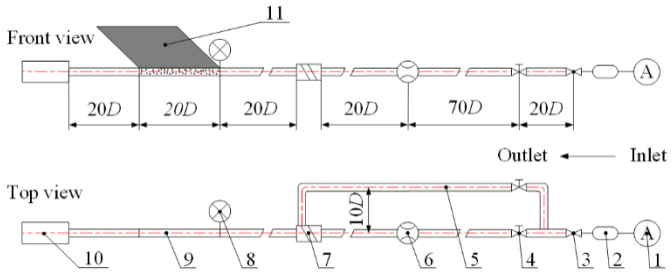

Figure 3. Schematic figure of the experimental setup. 1—Air compressor, 2—gas tank, 3—spherical valve, 4—spherical value, 5—tangential flow, 6—flowmeter, 7—swirling generator, 8—pressure sensor, 9—acrylic transparent tube, 10—receiving device, 11—high speed camera.

Figure 4 showed a cross-sectional view of a swirling generator. Three swirling blades were arranged to avoid the swirl decay in the case of too many blades. By changing the

regulating sleeve, the swirling number of the swirling flow could be adjusted accordingly. In the experiments, the total airflow varied from 40 m^3/h to 180 m^3/h. The typical ratio between the gas nozzle and the main inlet of the swirling generator was the ratio between the gas flow into the nozzle 12 as shown in Figure 4 and the total airflow. In each group of experiments, we kept the total inlet flow fixed. By changing the typical ratio, we could achieve different swirling numbers in the pneumatic conveying. The swirling intensity was adjusted by adjusting the size of the tangential flow valve, and the tangential flow ratio varied from 0–1 (see Table 2).

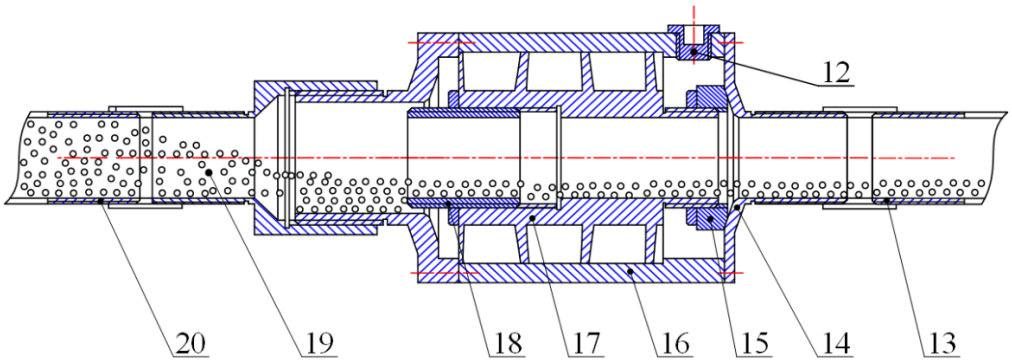

Figure 4. Split view of swirling generator [6]. 12—Gas nozzle, 13—inlet pipe, 14—right cover, 15—adjusting ring, 16—housing, 17—swirling blade, 18—regulating sleeve, 19—pebble particles, 20—outlet pipe.

Table 2. Experimental setup.

Value	Particle Size (mm)	Airflow (m^3/h)	Tangential Flow Ratio
Numerical value	3–5, 5–7, 7–9, 9–11, 11–13, 13–15	40–180	0–1

A vortex flowmeter and weighing sensor were used to achieve the airflow rate and particle mass, respectively, and the swirl number (S_N) could be defined as [14,15,21,23]:

$$S_N = \frac{\int_0^R 2\pi\rho_a u w r^2 \mathrm{d}r}{\int_0^R 2\pi\rho_a R u^2 r \mathrm{d}r} \quad (1)$$

where u and w are the axial and tangential velocities, respectively, and r is the radius of the pipe.

The experiments were implemented in a horizontal transparent pipe having a length of 1 m, the total mass of pebble material used in each experiment was 500 g, and the pebble material was tiled horizontally at the bottom of the pipeline having a tiling length of 500 mm. A fixed airflow rate was applied to the granular layer through the inlet of the pipeline. The particles accumulated in the transparent acrylic tube changed from static to rolling, sliding, or suspended under the airflow. The initial motion state and pickup process of pebble particles were recorded by a high-speed camera namely JVC/gc-px100bac, with a 500 FPS high-speed film recording capacity, and 500 FPS was used for experiment recording. In the experiments, the particles picked up by the airflow were collected through a porous filter that allows the airflow to pass but the particles. The masses of the picked particles were obtained by an electronic balance with a range of 2 kg, and its resolution was 0.01 g. Finally, the pickup velocity of the particles was calculated according to the 50% mass loss of pebble particles under different airflow rates.

3. Results and Discussion

3.1. Airflow Distribution

The airflow velocity is one of the key parameters that affect the flow pattern of the two-phase flow, and it is important to study the airflow distribution in horizontal pipelines.

Figure 5 shows the measurement area of the axial and tangential velocity distribution in the horizontal pipe; and the area was divided into five spaces from the top to the bottom. The axial airflow velocity was that along the positive direction of the z-axis, and the tangential airflow velocity is the positive direction along the y-axis. To reduce the errors caused by accidental experiments, the airflow velocities were measured thrice, and their average value was taken as the final result.

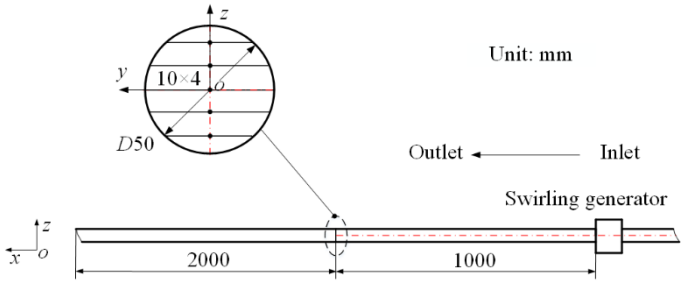

Figure 5. Schematic of experimental measuring domain.

Thermal anemometer AR866 was selected as the anemometer in the experiments, and its measuring range was 0.3–60 m/s with a resolution of 0.01 m/s. The measured airflow rates were those under standard conditions. To measure the axial airflow velocity, a flow of 200 m^3/h under standard conditions was chosen as the velocity measurement target.

Figure 6 shows the airflow distribution of the axial velocity (z-direction), and the color lines are the Gaussian fitting for different swirl numbers. For different swirl intensities, the axial flow velocities in the lower part of the pipeline are larger, whereas those in the upper part are smaller, which are attributed to gravity and the swirling generator. The axial speed of the flow increases first and then decreases with the swirl numbers. When the swirl number is S_N = 0.3, the axial speed reaches a maximum value of 41 m/s. With the increasing swirl number, the axial velocity of the pipe gradually decreases. This is because the axial velocity decreases with the swirl number, whereas the total flow remains unchanged, and the friction between the swirl flow and the wall intensifies. Compared with the axial flow, the swirl decay is more significant, and thus, the axial velocity decreases.

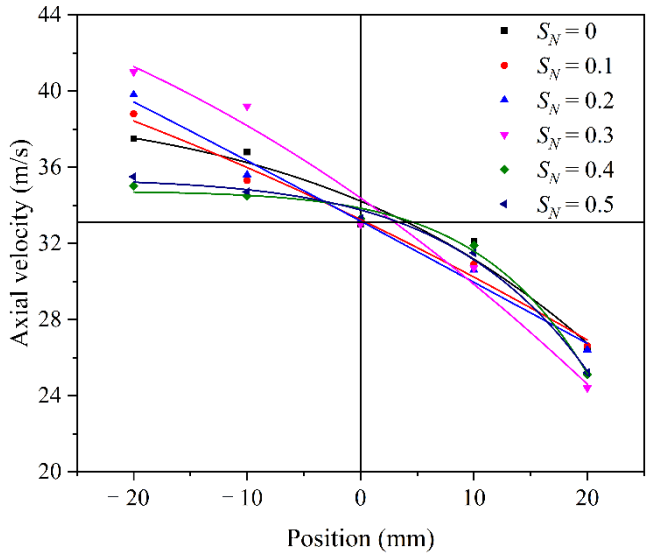

Figure 6. Axial airflow distribution and Gauss fitting under different swirl numbers.

Figure 7 shows the distribution of the tangential airflow velocity (y-direction), and the color lines are the Gaussian fitting for different swirl numbers. The airflow velocity along the positive y-axis is the positive direction, and the negative direction indicates

that the airflow velocity is along the negative the y-axis. The trends of the tangential and axial velocities are the same, and the tangential velocity in the upper part of the pipe is significantly smaller than that in the lower part of the pipe. The swirling generator plays an important role in airflow distribution.

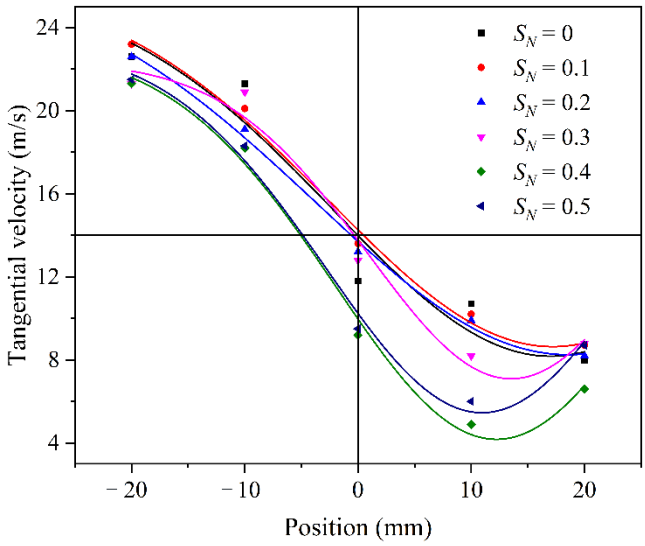

Figure 7. Tangential airflow distribution under different swirl numbers.

Furthermore, Figure 7 shows that with the increasing swirl number, the tangential velocity of the airflow increases gradually. However, the tangential velocity reaches a maximum with a swirl number of 0.3, indicating that when the swirl number is 0.3, the tangential swirl intensity in the horizontal pipe is the highest. It is found that the swirl number plays an important role in the swirling decay, the larger the airflow velocity is, the greater the swirl decay is, and the tangential airflow velocity will decrease accordingly. When the swirl number reaches 0.5, a lowest tangential airflow velocity is found. Simultaneously, the growth trend of the velocity near the wall of the pipeline is weakened, and presents a downward trend. This is because the velocity near the wall is less than that at the central axis owing to the friction between the wall and airflow.

3.2. Particle Pickup in Axial Flow

The experiments were implemented in a horizontal transparent pipe having a length of 1 m; the total mass of the pebble material in each test was 500 g, and was tiled horizontally at the bottom of the pipeline having a tiling length of 500 mm. A fixed airflow rate was applied to the granular layer through the inlet of the pipeline. The granular layer was picked up by airflow entrainment, and the surface airflow velocity was larger than the inlet velocity. As the particle layer eroded and gradually picked up, the average airflow velocity at the particle surface layer decreased (the cross-sectional area of the airflow increased), and the airflow velocity at the particle surface was calculated by dividing the volume airflow rate of the pipeline (free cross-sectional area), as shown in the following equation:

$$v_{sf} = v_{in}\frac{\pi r^2}{\pi r^2 - \frac{m_e}{\rho_b L_e}} = v_{in}\frac{\pi \rho_b L_e r^2}{\pi \rho_b L_e r^2 - m_e} \quad (2)$$

where v_{sf} is the airflow velocity on the particle surface, v_{in} is the inlet airflow velocity, m_e is the total mass of particles in each test, L_e is the particle layer length that were tiled, and ρ_b is the particle bulk density.

In the picking process of the 3–5 mm particles, the airflow at the inlet was 137–140 m^3/h, and the picking process of pebble particles in the horizontal pipe was recorded by using a high-speed camera, as shown in Figure 8. When t = 0.00 s, the particles remain still.

With time, the particles on the surface of the particle layer are gradually picked up. When t = 0.05 s, two protruding particles are picked up. The main reason is that the windward side of the particles is considerably large, and the horizontal force on the particles increases. When the force of airflow exceeds the friction force of the particles, the particles are picked up, begin to roll, and picked up again. As the laying of particles at the bottom of the pipeline is significantly affected by random factors, and the friction between the particle and wall, friction between particle and particle, particle size, and particle bulk density has a certain effect on the picking of pebble particles, the particles sometimes stop moving again after being picked up, as shown in Figure 8b. In this stage, only the particles with an uneven surface are forced more in the wind, and few particles are picked up. Therefore, to avoid the random influence of these factors on the picking of pebble particles, each test was performed twice. If the mass error of the two tests exceeded 20%, the test was conducted three or even four times. The singular test results were filtered out, and the average value of several groups of test picking was obtained.

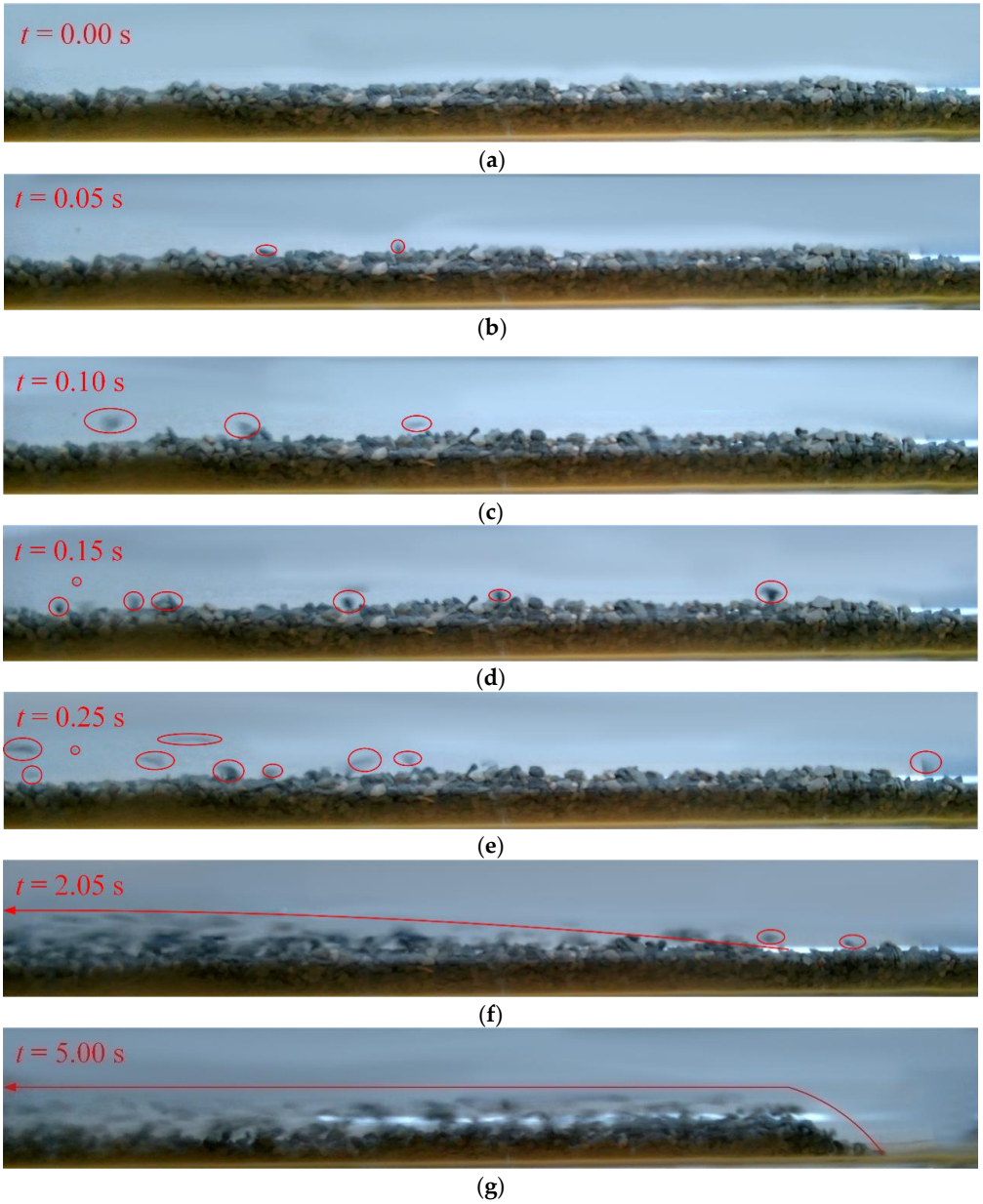

Figure 8. Pick-up process of pebble particles. (**a**) t = 0.00 s, (**b**) t = 0.05 s, (**c**) t = 0.10 s, (**d**) t = 0.15 s, (**e**) t = 0.25 s, (**f**) t = 2.05 s, (**g**) t = 5.00 s.

Figure 8 depicts that particle-picking starts with a few particles rolling and impacting other particles, and the particles at the end of the pipeline are picked up gradually and suspended. When the particles are reduced to a certain number, the particles move in the form of laminar flow. The picking process can be divided into four stages. First, particles begin to roll along the particle layer (Figure 8b). Second, the picked particles collide with other particles in the layer (Figure 8c–e), and the particles begin to rebound. Third, the newly picked particles collide with the particles already carrying air (Figure 8f). Fourth, the windward side of the particle group is picked up gradually, and the particle-picking process ends.

It can be seen from Figure 8c–f that as few particles are picked up, the picked-up particles roll and jump, thereby impacting the deposited particles, and these particles are picked up (as shown in Figure 8c–e). The picked-up particles impact other particles in the rolling process, causing the particles on the surface of the particle group to be picked up gradually. The picking process of the particle group gradually slows down with cutting, as shown in Figure 8f. With the picking process, the number of particles deposited at the bottom gradually decreases, and the friction between the particles and the wall decreases. When the fluid force on the windward side of the particles exceeds the friction of the particle pile, the particles move along the outlet in the form of laminar flow, as shown in Figure 8g.

Some randomness exists in the particle-picking process; thus, the particle-picking regimes will appear in a limited range of airflow velocity only. Therefore, the pickup velocity of the particles determined by visual observation will lead to a certain error, and a reasonable pickup velocity is a key to the research on the process of particle-picking in horizontal pipes; some researchers had a different definition of pickup velocity in the past. To solve the problem of micro-particle dune flow, Hayden et al. [26] slanted the material inside the pipe and made it away from the air source. They inferred the pickup velocity of particles inversely by measuring the height of the stabilized particle group and made the airflow velocity when the mass of particles picked up was larger than zero be the pickup velocity of materials. Kalman et al. [12] defined the mass loss of particles within 30 s in one test, and the pickup velocity was identified as the airflow velocity when the material mass loss was not zero. Rabinovich [27] and Zhou [12] defined the airflow velocity when the picking mass of the particle was 50% as the pickup velocity. To reduce the influence of random factors on the pickup velocity, this paper tended to measure the pickup velocity qualitatively, the pickup velocity of pebble particles was determined by drawing the function relationship between the airflow and the entrainment of particles, measuring the intersection point of measurement point and vertical coordinate as well, the pickup velocity was treated as the airflow velocity when the picking mass was 50%. Based on the function relation of the mass loss, higher measurement accuracy could be obtained. The greater the number of particles measured, the higher the measurement accuracy.

Figure 9 shows the functional relationship between the pickup velocity of pebble particles with different sizes and airflow velocities. The picking rate is selected as the measurement index of the pickup velocity, that is, the ratio of the picking mass to the total mass of the material. The pickup ratios are low at low airflow velocity for different sizes due to the solid pickup velocity, and then a large number of particles are picked up in a small velocity range. For pebble particles with different particle sizes, the 50% pickup velocities are 17.9 m/s, 20.5 m/s, 22.1 m/s, 20.7 m/s, 17.0 m/s, 19.5 m/s, respectively. When particle pickup begins, the picking rate of the particles has an approximately linear relationship with the airflow velocity. For various sizes of pebble particles, the bulk density decreases with the particle size, resulting in the increasing of the porosity. The larger the particle size, the higher the accumulated height of the particles, which will increase the surface airflow velocity of the particles. Rabinovich et al. [27] found that the maximum pressure drop above the particle accumulation is equal to 10% when the accumulation at the bottom was less than 70%. They considered that the effect of particle accumulation on particle-picking can be ignored. However, when the sediment height exceeds 90% of the

pipeline, the calculation of the pickup velocity may lead to errors that cannot be ignored. The effects of the airflow velocity, material permeability, and particle stacking height should be considered.

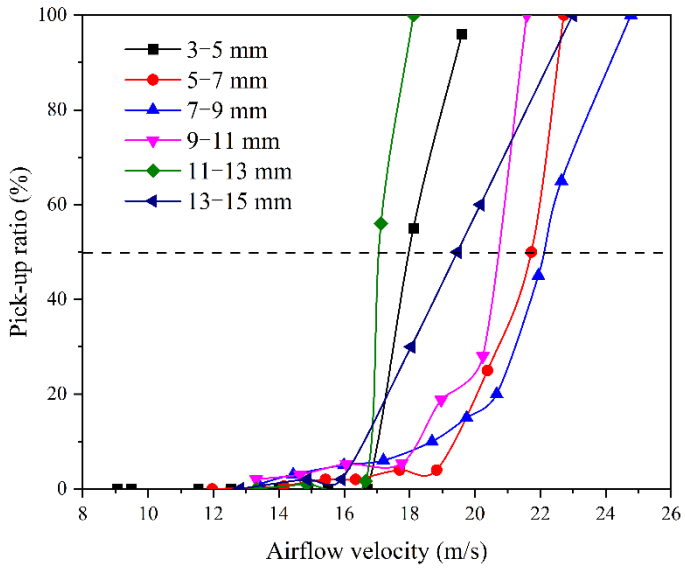

Figure 9. Pick-up ratio of pebble particles with different particle sizes.

Figure 10 shows the pickup velocity of pebble particles with a picking rate of 50% for particles with different particle sizes. For particles from 3 to 9 mm, the pickup velocity increased with the increasing size, which is consistent with the research results of Kalman, Rabinovich, and Zhou et al. [12,27]. As regards the size of particles in a specific range, Kalman's empirical equation was more suitable for the prediction of the particle pickup velocity of the particles considered in this study. For particles ranging from 9–11 mm, the surface airflow velocity and the height of the windward side had significant effects on particle-picking, and the pickup velocity of the particles was low. For pebble particles of 5–9 mm, the pick-up masses were the minimum. Therefore, for pneumatic conveying of the gas-solid two-phase flow, it was often required that the particle size was less than three times the pipe diameter. When the particle size was close to 1/3 of the pipe diameter, the particle would not be suitable for conveying in such a small pipe.

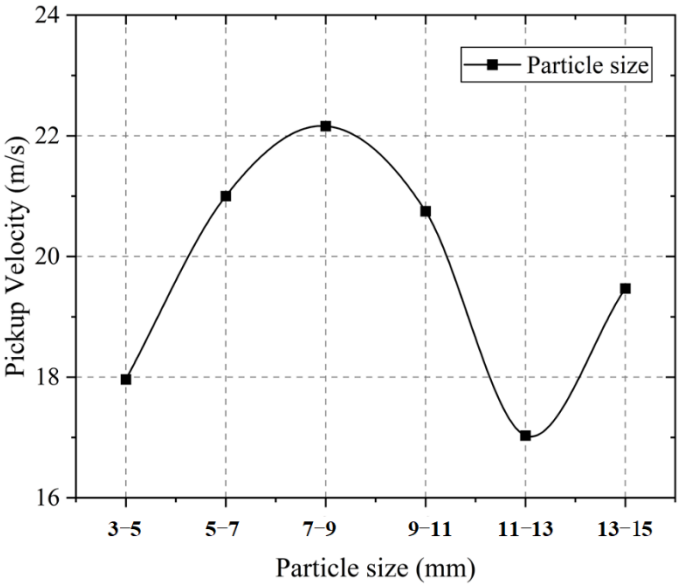

Figure 10. Function between particle size and pick-up velocity.

The stress analysis of a particle in the axial flow field of a horizontal pipeline is shown in Figure 11. In the figure, u_a is the airflow velocity vector, u_p and ω_p are the velocity the vector and angular velocity vector of spraying particles respectively. According to the gas–solid two-phase hydrodynamics, the forces received by spraying particles when moving in the flow field include the gravity, the drag force generated by the relative velocity between airflow, the lift force generated by the particles rotation, and pressure gradient force generated by the velocity difference between the upper side and lower side of the particles and pressure gradient force, buoyancy force and other forces generated by temperature difference and electric field. The above forces have different effects on particle motion in different airflow. In the pneumatic conveying system of spraying particles, there is a great difference between the particle density and the gas density, and the size of a single spraying particle is large. Among the above forces, only the drag force, rotating lift force and particle inertia force are of the same order of magnitude and have an impact on the movement.

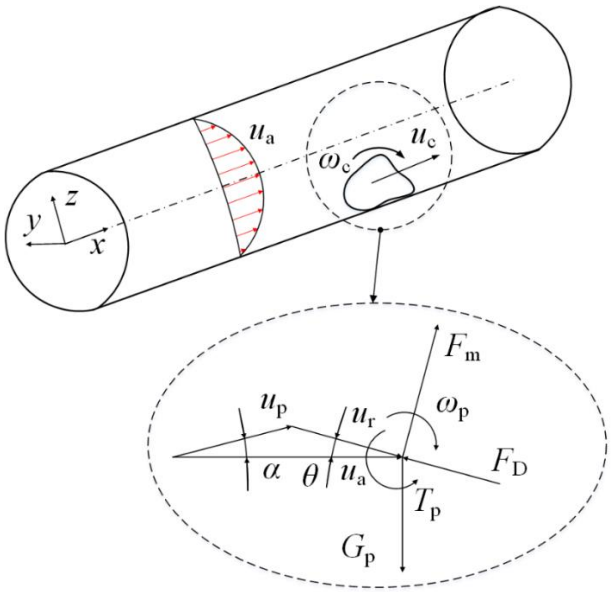

Figure 11. Forces analysis of single spraying particle in horizontal axial pneumatic conveying.

When measuring the dispersion of different data, directly comparing the two groups of data with the standard deviation will lead to a large error. Comparing with CV can eliminate the influence of measurement scale and size. The CV is the ratio of the standard deviation of the original data to the average value, as shown in Equation (3). There are no dimensions, so objective comparisons can be made.

$$\mathrm{CV} = \frac{\sigma_x}{E_x} \tag{3}$$

where CV is the coefficient of variation, σ_x is the standard deviation, E_x is the average.

Figure 12 shows the normalized functional relations between the airflow velocity and the CV of the pressure under different particle sizes. In this study, because the end of the test pipeline was a free flow outlet, the pressure of the pressure transmitter could be regarded as the pressure drop of the tested pipeline. CV can be used to describe the fluctuation of the flow field in a horizontal pipeline. The larger the CV, the more unstable the flow field. For particle multiphase flow, particle pickup and suspension affect the stability of the flow field. Therefore, CV is selected as another index to measure the pickup velocity.

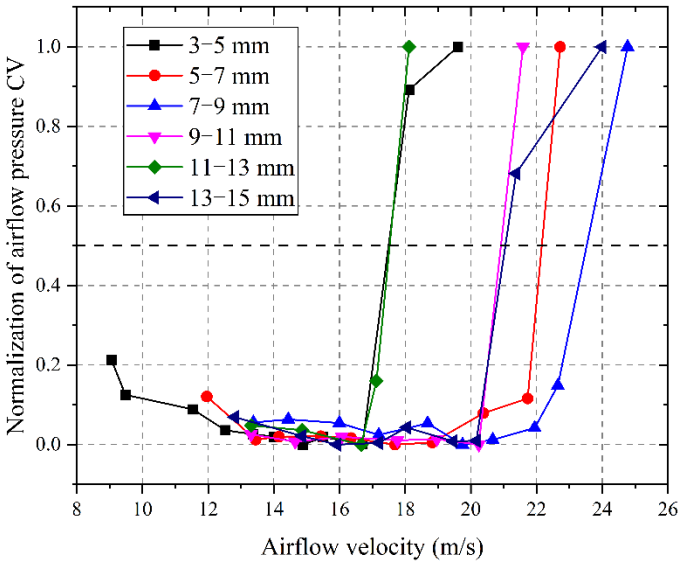

Figure 12. Relationship between coefficient of difference and airflow velocity.

For lower airflow velocity, the CV of the airflow pressure is low, which is less than 0.2. This is mainly because the airflow velocity is less than the particle pickup velocity, so only a few particles are picked up at this low airflow velocity. The fluctuation of the flow field is caused by the decrease in the ventilation cross-sectional area of the flow field caused by the particle pile, and the periodic acceleration and deceleration of the airflow caused the fluctuation of the gas. With the increasing airflow velocity, the particles begin to be picked up, and the pressure CV increases gradually. For the pebble particles of 3–9 mm, with the increasing particle size, the airflow velocity will be larger, which is similar to the result of the picking rate measurement index. Furthermore, no linear relationship exists between the CV of the pressure and particle size with sizes of 9–11 mm, 11–13 mm, and 13–15 mm. When the particle size exceeds 9 mm, the particle pickup velocity is smaller than that of the 7–9 mm particles. One reason is that with the increasing particle size, the porosity of particles increases, the packing density of particles decreases, the permeability of particles increases, and large particles tend to be disturbed and picked up by airflow. In addition, for horizontal pneumatic conveying with fixed pipe diameter, the surface airflow velocity of the large particles is higher; thus, the pickup velocity will be smaller.

Some errors may exist when the particle pickup velocity is measured using the CV of a flow field if the time of particle-picking is substantially long or the particle-picking process may be completed in an instant or within a period. Therefore, the PAR is adopted to further optimize the pickup velocity obtained by the CV in this study, as shown in the following equation:

$$r_{par} = \frac{x_{i,\max}}{E_X} \tag{4}$$

where r_{par} is the peak-average ratio of the pressure drop, $x_{i,\max}$ is the peak pressure signal, and E_x is the average of the pressure drop.

Figure 13 shows the normalized function between the airflow velocity and PAR under the pipeline pressure of particles of different sizes, it can be seen from the figure that the relation of PAR has a certain similarity with the function of CV, the pickup velocities obtained by taking 50% of the PAR as the calculation are 17.54 m/s, 22.17 m/s, 22.51 m/s, 20.95 m/s, 17.57 m/s, and 22.74 m/s respectively, which are approximately equal to the pickup velocity obtained by taking the CV as the measurement index in Figure 13. For particles of 13–15 mm, the pickup velocity obtained by taking the PAR as the measuring index is higher than those obtained by using the CV, and the pickup velocity is closer to that obtained by using the picking volume, therefore, the pickup velocity of the particles can be accurately obtained by using the PAR within a certain range.

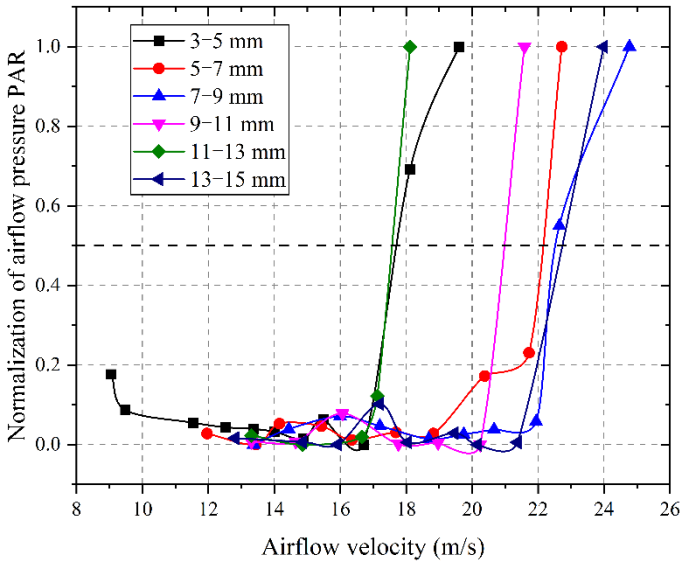

Figure 13. Relationship between peak-to-average rate and airflow velocity.

By comparing Figures 9, 12 and 13, the airflow velocity present the same effect for particle pickup mass, airflow pressure CV, and PAR. In other words, for pipeline pneumatic conveying which is not conservative for the measurement of the material pickup rate, the particle pickup velocity, and optimal swirl number can be obtained by determining the pressure characteristics of the flow field, CV of the pressure signal, and PAR. When the pickup quality is used to evaluate the pickup velocity, the accuracy is the highest, the pressure CV is the second, and par is the worst.

3.3. Particle Pickup in Swirling Flow

It was found from the results of the pure axial flow experiment that the pickup velocity of particles with a particle size of 3–9 mm exhibited a linear relationship. Therefore, pebble particles with particle sizes of 3–5 mm, 5–7 mm, and 7–9 mm were selected as the test objects for flow transportation in the swirling flow field, as shown in Equation (1); when the total flow remains constant as the premise, by changing the swirl number, the pickup velocity of pebble particles under different swirl numbers can be obtained, as shown in Figure 14.

As seen in Figure 14a, for pebble particles of 3–5 mm, when the total airflow velocity is lower than 17.54 m/s, the S_N has an insignificant effect on the particle pickup velocity and instead has an inhibiting effect. With the increasing inlet airflow velocity, a relatively lower swirl number promotes the particle-picking process. When the swirl number is between 0.1 and 0.2, the particle pickup rate reaches the maximum, whereas, with the increasing swirl number, the particle pickup rate decreases gradually owing to the swirl decay. For particles having sizes of 5–7 mm and 7–9 mm and low airflow velocity, as shown in Figure 14b,c, the swirl number has no significant effect on the pickup rate; however, when the airflow velocity is almost similar to the pickup velocity, the swirl number seriously affects the particle-picking ratio. When the swirl number is between 0.1 and 0.2, the pickup rate of particles is the largest, which is similar to the pebble particle swirl conveying with a size of 3–5 mm, that is, the best swirl number exists, and the pickup rate of materials is the largest.

For the swirling pneumatic conveying, the spin motion of spraying particles in the transportation process can be ignored, but the spiral motion of particles around the pipeline axis cannot be ignored. The stress analysis of a single particle in the horizontal pipeline swirling field is shown in Figure 15. In the axial direction, the spraying particle is only affected by the axial drag of the airflow, and in the tangential direction, the particle is affected by gravity, drag, and centrifugal force.

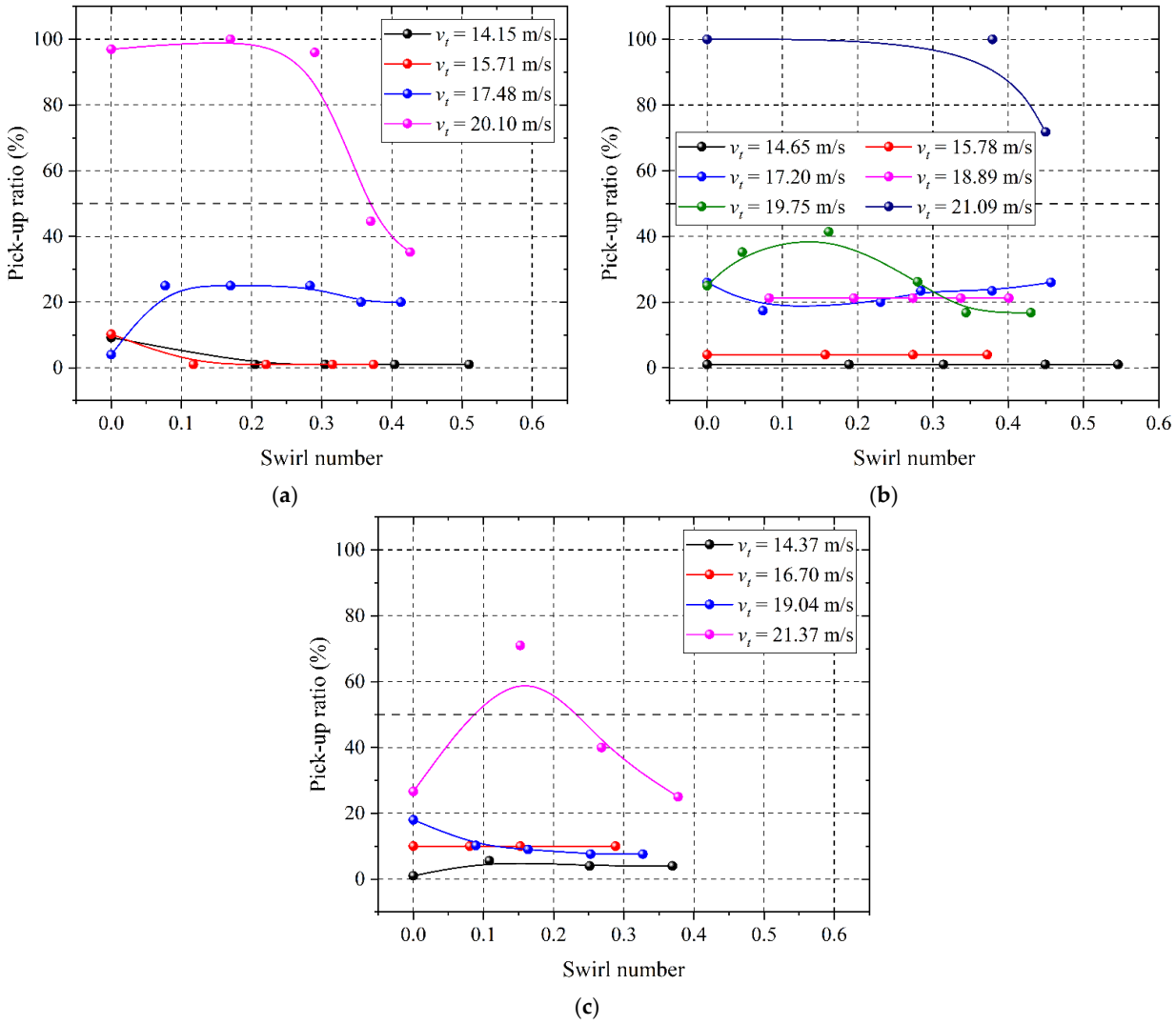

Figure 14. Effect of swirl number on picking velocity of pebble particles. (**a**) d_p = 3–5 mm, (**b**) d_p = 5–7 mm, (**c**) d_p = 7–9 mm.

For pebble particles with large sizes, the pickup velocity differs significantly from that of small particles, mainly because large particles have better air permeability, lower pack-density between particles, and a more significant disturbance effect of swirling flow on the particle group, making it easier for the particles to be picked up. A larger swirl number is not conducive to particle pickup, which is mainly because of the swirl decay. Increasing the swirl number means reducing the axial airflow velocity. Although the tangential flow is conducive to particle disturbance, there will be an optimal swirl number in the process of particle pickup due to the large friction loss energy between the tangential flow and the pipe wall.

Therefore, the swirling velocity can be estimated by using the following equation:

$$v_{pu,s} = \left[-a_s\left(x - S_{N,op}\right)^2 + b_s\right]v_{pu},\ v_{pu} < f\left(d_{p,i}/d_{p,1}\right)v_{in} \tag{5}$$

where $v_{pu,s}$ is the particle pickup velocity under the swirling flow, a_s and b_s are constants associated with conveying materials, and they are all larger than 0, and $S_{N,op}$ is the swirl number corresponding to the maximum pickup rate. For the pebble particles investigated in this study, $0.1 < S_{N,op} < 0.2$ $f\left(d_{p,i}/d_{p,1}\right)$ is a function related to the particle size, and v_{in} is the inlet airflow velocity.

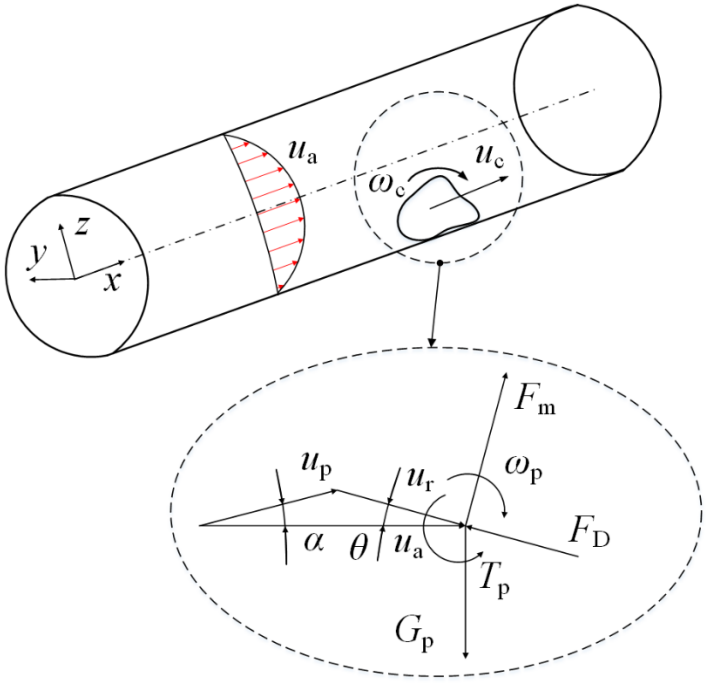

Figure 15. Forces analysis of single spraying particle in horizontal swirling pneumatic conveying.

Figure 16 shows the normalization between the airflow velocity and the pressure CV of the swirling pneumatic conveying. It can be seen from the figure that when the airflow velocity was smaller than the particle pickup velocity, the CV of the flow pressure was relatively low, and they were all less than 0.2. With the increasing swirl number, the CV decreased gradually. This indicated that the particle on the flow field was progressively weakened, and only a small amount of particles were picked up. For pebble particles with a grain size of 3–9 mm, when the airflow velocity was close to the pickup velocity, the particles began to be picked up with the swirl number, and it reached the maximum when the swirl number was 0.1–0.3. With continuously increasing the swirl number, the CV of flow pressure drop decreased due to the swirl decay. Compared with the measurement index of pickup rate, the results of the CV had a certain similarity with the former, which meant that the particle pickup regimes can also be obtained qualitatively by measuring the CV of airflow pressure in horizontal pipelines.

Figure 17 shows the normalization between the airflow velocity and the PAR. The PAR has a high similarity with the pickup velocity obtained from the particle pickup rate results and CV results, and the PAR reaches its maximum value at a swirl number of 0.1–0.3. The PAR of pressure in the flow field is highly reliable as the pickup index of swirling pneumatic conveying, the pickup velocities obtained by the PAR as the measuring index are more accurate than the CV, and the pickup velocity is closer to those obtained by pickup rate.

Comparing the pure axial flow field with the swirl flow field, the accuracy of particle pickup velocities obtained by visual observation is the worst, and it reaches the best when the particle mass loss rate of selecting is selected as the index. For particle conveying which is not convenient to measure the particle pickup ratio, the particle pickup velocity, and the optimal swirl number could be obtained qualitatively by measuring the airflow pressure drop, the CV of pressure signals, and the PAR.

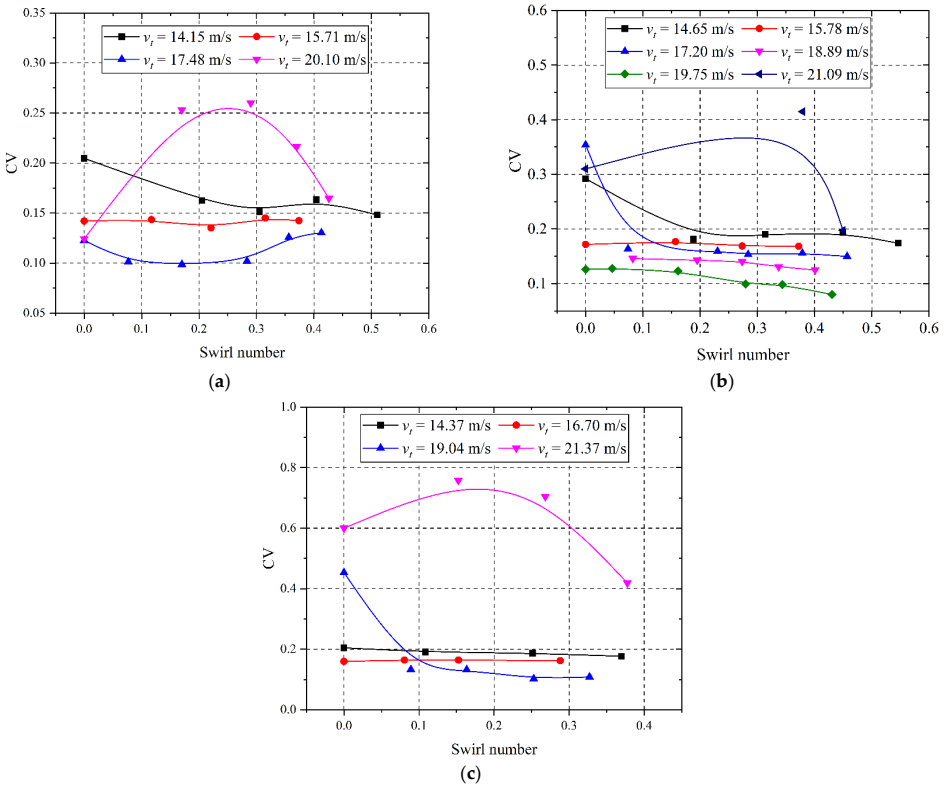

Figure 16. Effect of swirl number on coefficient of variation of pebble particles. (**a**) d_p = 3–5 mm, (**b**) d_p = 5–7 mm, (**c**) d_p = 7–9 mm.

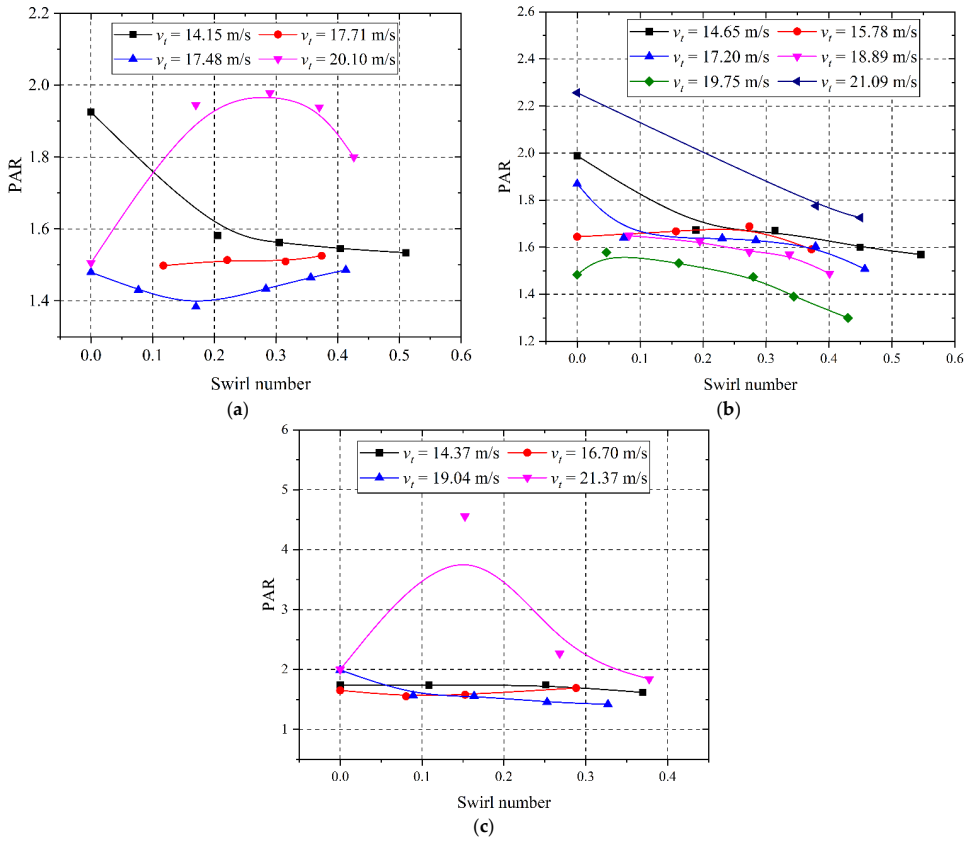

Figure 17. Effect of swirl number on peak to average ratio of pebble particles. (**a**) d_p = 3–5 mm, (**b**) d_p = 5–7 mm, (**c**) d_p = 7–9 mm.

4. Conclusions

The pickup velocity of the pebble particles selected in this experiment was studied based on an empirical analysis of the particle pickup velocity and existing research results. The airflow velocity is found to appropriately describe all the results as a function of the pickup velocity, and a good correlation exists between them. Furthermore, it is found that the experimental object was suitable for the Kalman empirical equation when the range of the particle size is 3–9 mm, and the pickup velocity increased with the particle sizes. Large particles have larger windward surface areas and voidage, and their pickup velocity is affected by the particle size and the internal size of the pipeline.

For pebble particles with large sizes, the pickup velocity is significantly different from that of small particles, and this is mainly attributed to the influence of the windward surface area and particle voidage of large particles. When the swirling flow number ranges from 0.1–0.2, the particle-picking rate reaches the maximum. When the particle pickup velocities obtained by using four methods, namely, visual observation, mass weighing, analysis of the CV of the pressure drop in a flow field, and determination of the PAR of the pressure drop in the flow field, were compared, the results showed that the accuracy of the particle pickup velocity obtained through visual observation was the lowest, and that obtained by selecting the particle mass-loss rate as the measurement index was the highest. For pipeline pneumatic conveying, which is not convenient for the measurement of the material pickup rate, the particle pickup velocity and optimal swirl number can be obtained by determining the pressure characteristics of the flow field, CV of the pressure signal, and PAR.

Author Contributions: Y.J.: conceptualization, project administration, writing—original draft, funding acquisition; Y.H.: writing—review and editing, methodology; N.Y.: investigation, formal analysis; T.G.: investigation; D.G.: writing—review and editing; Y.L.: writing—review and editing. All authors have read and agreed to the published version of the manuscript.

Funding: This research was funded by National Natural Science Foundation of China (grant number 52005430) and Natural Science Foundation of Hebei Province (grant number E2021203108).

Institutional Review Board Statement: Not applicable.

Informed Consent Statement: Not applicable.

Data Availability Statement: Not applicable.

Acknowledgments: This study was supported by the National Natural Science Foundation of China (Grant No. 52005430), and the Natural Science Foundation of Hebei Province (Grant No. E2021203108), which are all gratefully acknowledged.

Conflicts of Interest: No potential conflict of interest was reported by the authors.

Nomenclature

S_N	Swirl number	-	u	Airflow axial velocity	m/s
R	Pipe radius	m	w	Airflow tangential velocity	m/s
ρ_a	Gas density	kg/m^3	v_{sf}	Particle surface airflow velocity	m/s
v_{in}	Inlet airflow velocity	m/s	m_e	Each test particle mass	kg
ρ_b	Particle bulk density	mm	L_e	Particle layer length	m
CV	Coefficient of variation	-	E_x	Mean value	kPa
σ_x	Standard deviation	kPa	R_{par}	Peak-average ration	kPa
$X_{i,max}$	Peak pressure	kPa	$v_{pu,s}$	Swirl pickup velocity	m/s
a_s	constant	-	b_s	constant	-
v_{pu}	Pickup velocity	m/s	$S_{N,op}$	Maximum pickup swirl number	-
r_{xx}	Auto-correlation function	kPa	n	Sequence length	-

References

1. Zhang, Z.; Zhang, R.; Cao, Z.; Gao, M.; Zhang, Y.; Xie, J. Mechanical Behavior and Permeability Evolution of Coal under Different Mining-Induced Stress Conditions and Gas Pressures. *Energies* **2020**, *13*, 2677. [CrossRef]
2. Cheng, L.; Ge, Z.; Chen, J.; Ding, H.; Zou, L.; Li, K. A Sequential Approach for Integrated Coal and Gas Mining of Closely-Spaced Outburst Coal Seams: Results from a Case Study Including Mine Safety Improvements and Greenhouse Gas Reductions. *Energies* **2018**, *11*, 3023. [CrossRef]
3. Beaulac, P.; Issa, M.; Ilinca, A.; Brousseau, J. Parameters Affecting Dust Collector Efficiency for Pneumatic Conveying: A Review. *Energies* **2022**, *15*, 916. [CrossRef]
4. Dudić, S.; Reljić, V.; Šešlija, D.; Dakić, N.; Blagojević, V. Improving Energy Efficiency of Flexible Pneumatic Systems. *Energies* **2021**, *14*, 1819. [CrossRef]
5. Ji, Y.; Liu, S.; Jia, J.; Yao, J. Analysis of the pick-up of crushed stone particles in a horizontal pipeline. *Powder Technol.* **2021**, *377*, 534–544. [CrossRef]
6. Ji, Y.; Hao, Y.; Yi, N.; Guan, T.; Gao, D. Particle flow regime in a swirling pneumatic conveying system. *Powder Technol.* **2022**, *401*, 117328. [CrossRef]
7. Marcus, R.D.; Leung, L.S.; Klinzing, G.E.; Rizk, F. *Pneumatic Conveying of Solids*; Springer: Dordrecht, The Netherlands, 2010.
8. Soepyan, F.B.; Cremaschi, S.; Sarica, C.; Subramani, H.J.; Gao, H. A model ranking and uncertainty propagation approach for improving confidence in solids transport model predictions. *J. Petrol. Sci. Eng.* **2017**, *151*, 128–142. [CrossRef]
9. Rice, H.P.; Fairweather, M.; Peakall, J.; Hunter, T.N.; Mahmoud, B.; Biggs, S.R. Constraints on the functional form of the critical deposition velocity in solid–liquid pipe flow at low solid volume fractions. *Chem. Eng. Sci.* **2015**, *126*, 759–770. [CrossRef]
10. Gomes, L.M.; Mesquita, A.L.A. Effect of particle size and sphericity on the pickup velocity in horizontal pneumatic conveying. *Chem. Eng. Sci.* **2013**, *104*, 780–789. [CrossRef]
11. Dasani, D.; Cyrus, C.; Scanlon, K.; Du, R.; Rupp, K.; Henthorn, K.H. Effect of particle and fluid properties on the pickup velocity of fine particles. *Powder Technol.* **2009**, *196*, 237–240. [CrossRef]
12. Kalman, H.; Satran, A.; Meir, D.; Rabinovich, E. Pickup (critical) velocity of particles. *Powder Technol.* **2005**, *160*, 103–113. [CrossRef]
13. Zhou, J.; Xu, L.; Du, C. Prediction of lump coal particle pickup velocity in pneumatic conveying. *Powder Technol.* **2019**, *343*, 599–606. [CrossRef]
14. Zhou, J.; Du, C.; Ma, Z. Influence of swirling intensity on lump coal particle pickup velocity in pneumatic conveying. *Powder Technol.* **2018**, *339*, 470–478. [CrossRef]
15. Zhou, J.; Du, C.; Liu, S.; Liu, Y. Comparison of three types of swirling generators in coarse particle pneumatic conveying using CFD-DEM simulation. *Powder Technol.* **2016**, *301*, 1309–1320. [CrossRef]
16. Ibrahim, K.A.; Hamed, M.H.; El-Askary, W.A.; El-Behery, S.M. Swirling gas-solid flow through pneumatic conveying dryer. *Powder Technol.* **2013**, *235*, 500–515. [CrossRef]
17. Yao, S.; Fang, T. Analytical solutions of laminar swirl decay in a straight pipe. *Commun. Nonlinear Sci.* **2012**, *17*, 3235–3246. [CrossRef]
18. Fokeer, S.; Lowndes, I.S.; Hargreaves, D.M. Numerical modelling of swirl flow induced by a three-lobed helical pipe. *Chem. Eng. Processing Process Intensif.* **2010**, *49*, 536–546. [CrossRef]
19. Fokeer, S.; Lowndes, I.; Kingman, S. An experimental investigation of pneumatic swirl flow induced by a three lobed helical pipe. *Int. J. Heat Fluid Fl.* **2009**, *30*, 369–379. [CrossRef]
20. Hui, L.I.; Tomita, Y. Measurements of Particle Velocity and Concentration for Dilute Swirling Gas-Solid Flow in a Vertical Pipe. *Particul. Sci. Technol.* **2002**, *20*, 1–13.
21. Li, H.; Tomita, Y. A Numerical Simulation of Swirling Flow Pneumatic Conveying in a Vertical Pipeline. *Particul. Sci. Technol.* **2001**, *19*, 355–368. [CrossRef]
22. Li, H.; Tomita, Y. Particle velocity and concentration characteristics in a horizontal dilute swirling flow pneumatic conveying. *Powder Technol.* **2000**, *107*, 144–152. [CrossRef]
23. Li, H.; Tomita, Y. An Experimental Study of Swirling Flow Pneumatic Conveying System in a Vertical Pipeline. *J. Fluids Eng.* **1998**, *120*, 200–203. [CrossRef]
24. Li, H.; Tomita, Y. An Experimental Study of Swirling Flow Pneumatic Conveying System in a Horizontal Pipeline. *J. Fluids Eng.* **1996**, *118*, 526–530. [CrossRef]
25. Zhou, L.X.; Chen, T. Simulation of swirling gas–particle flows using USM and $k-\varepsilon-k_p$ two-phase turbulence models. *Powder Technol.* **2001**, *114*, 1–11. [CrossRef]
26. Hayden, K.S.; Park, K.; Curtis, J.S. Effect of particle characteristics on particle pickup velocity. *Powder Technol.* **2003**, *131*, 7–14. [CrossRef]
27. Rabinovich, E.; Kalman, H. Incipient motion of individual particles in horizontal particle-fluid systems: A. Experimental analysis. *Powder Technol.* **2009**, *192*, 318–325. [CrossRef]